

Strain Rates in Prestressed Concrete Sleepers and Effects on Cracking Loads

Javad Taherinezhad*, Massoud Sofi, Priyan Mendis and Tuan Ngo

Department of Infrastructure Engineering, The University of Melbourne, Australia

javadt@student.unimelb.edu.au

ABSTRACT: Prestressed concrete sleepers (PCSs) play an essential role in structural response and performance of ballasted railway tracks. Due to defects in track or train components, high magnitude dynamic loads may generate at the rail head and transfer to the PCSs which can generate cracks in PCSs. Cracking from dynamic loads have been reported as the most critical problem of PCSs around the world and impose an early replacement of sleepers which is a financial burden to the rail industry. This paper investigates the effects of strain rates on the strength enhancement of PCS. By using available measurements, the strain rates are calculated at two critical points of the PCSs, the rail seat and midspan. Considering the dynamic increase factor (DIF) of concrete, the cracking loads of a PCS are calculated and are compared with commonly occurring dynamic loads. Results show that the maximum strain rates at both rail seat and midspan are about 0.08 and 0.016 1/s, respectively. The increase of cracking wheel load due to the strain rate effects is about 5 to 26 percent. The results are also shown to be able to demonstrate the level cracking from dynamic loads with very short return periods.

Keywords: *Concrete sleeper, Strain rate, Cracking loads, Dynamic Increase Factor.*

1 INTRODUCTION

Railway commonly provides the safest and the best transportation mode for both passenger and merchandise across the world. Conventional (ballasted) track consists of superstructure and substructure. The rails, rail pads, fastening systems and sleepers or ties make up the superstructure. The substructure consists of ballast, sub-ballast and formation layer. Distributing track loads from rail to ballast, sleepers play an essential role in track performance and safety. Now, prestressed concrete sleepers (PCSs), as the most commonly used types of sleepers (Okonta & Magagula, 2011), are popular and widely employed in many countries. With longer life cycle and lower maintenance costs, PCSs brought many technical and economic advantages to the railway engineering.

While the dead load of sleepers is typically considered as negligible, sleepers are subjected to dynamic loads generated due to wheel and rail interactions. In ideal conditions of the track and train wheels, the magnitude of these loads is low, but the repetition is high (high cycle). Nevertheless, the magnitude of loads may increase considerably in the existence of rail irregularities, wheel abnormalities or even support discontinuities, but the repetition of these loads is low (low cycle). Reviewing published

literature, Remennikov and Kaewunruen (Remennikov & Kaewunruen, 2008) found that the shape of dynamic loads in time domain varies with the sources and its magnitude significantly depends on the rolling speed. Further, it has been reported that the maximum magnitude of dynamic loads varies in the range of 100 to 750 kN, with a duration between 1 and 12 ms and a frequency range of up to 2000 Hz. The static axle loads, however, vary from 50 kN to 350 kN (Esveld, 2001).

An allowable stress approach which relies on simplistic impact factors is recommended by many standards such as Australia (AS-1085.14, 2012), USA (AREMA, 2006) and Europe (EN-13230-2, 2009), as a general design approach of PCSs and the railway track. However, few researchers have criticised the allowable stress method as conservative, unrealistic and inadequate to design and evaluate PCSs and have tried to develop a limit state design methodology which consider the dynamic aspects of loads and their effects on structural behaviour of PCSs (Remennikov, Murray, & Kaewunruen, 2007), (Leong & Murray, 2008) and (Nairn & Stevens, 2010).

To cover the lack of knowledge and to provide better understanding in the field of dynamic behaviour of PCSs, a vast number of experimental and numerical research works have been conducted through the last two decades. These works have led to identification

of the dynamic responses of PCSs and their interactions with other components of track, especially with ballast, rails and rail pads (for more information, see (Taherinezhad, Sofi, Mendis, & Ngo, 2013)). However, some structural aspects, such as strain rate effects and dynamic cracking behaviour, of PCSs are still lacking.

In this paper the influence of strain rate on cracking load of PCSs has been studied. Firstly, the effects of cracks on structural and durability behaviour of concrete are presented. Afterwards, the dependency of concrete behaviour, especially the tensile strength, on the strain rates is discussed based on the literature. Then, the levels of strain rates at both rail seat and midspan of a PCS are estimated based on strain variations in time domain that measured experimentally and published in the literature. For the next stage, a widely applied and well-studied sleeper has been optimised in length to obtain the maximum allowable axle load. Then, using a computer program, the magnitude of dynamic wheel loads which can cause crack initiation in the sleeper is estimated considering various parameters such as rolling speed, asymmetrical condition of loading and strain rate effects. The program has been developed to calculate both the tensile and compressive stresses of PCSs based on the design method prescribed by AS 1085.14 (AS-1085.14, 2012). Finally, the influence of strain rate on crack initiation of concrete is described.

2 CRACKING EFFECTS ON PCSS

PCSs are expected to withstand high magnitude dynamic loads and harsh environments. While service loads can lead to micro-cracks in PCSs, the high magnitude dynamic loads even with a few years return period could cause cracks to propagate over the half of sleeper height and appear as visible (Taherinezhad et al., 2013). For example, several investigations in Sweden have indicated that approximately 500,000 of 3 million visually inspected sleepers had macroscopic (visible) cracks (Thun, Utsi, & Elfgren, 2008). According to the worldwide survey which has been conducted by Van Dyk et al. (Van Dyk, Dersch, & Edwards, 2012), cracking has been ranked as the most critical problem of PCSs, especially those due to dynamic loads (**Error! Reference source not found.**).

Due to the use of prestressing requirements, high strength concrete (HSC) is often used to produce PCSs. The minimum compressive strength of concrete is restricted to 50 MPa in Australia (AS-1085.14, 2012) and 48.3 MPa (7,000 psi) in USA (Lutch, Harris, & Ahlborn, 2009). Owing to the variations in fracture modes and microstructure, HSC

is structurally a different material in comparison with normal strength concrete (NSC). The main concern regarding the use of HSC is the reduction in ductility with the increase in compressive strength (Mendis, 2001). Smooth fractures across micro-cracks and the lack of aggregate interlock are said to contribute to the brittle nature of HSC (Mendis, 2000). This brittleness may be the primary cause of cracking at PCSs that are highly subjected to dynamic loads.

Cracking of PCSs is a crucial factor, not merely in terms of mechanical and load carrying capability, but also for durability and fatigue properties. Further, the pattern and severity of cracks are essential factors in the assessment of sleepers. Though it is not unreasonable to consider cracking as the most important failure of PCSs.

2.1 Structural Effects

By conducting fatigue tests, Thun et al. (Thun et al., 2008) investigated the load carrying capacity of 13 sleepers which had been extremely cracked under real conditions of railway tracks. The sleepers have been subjected to 2 million cycles of loading (rail seat bending) based on the Swedish railway code. It is reported that only 6 sleepers passed through the test whilst 7 sleepers have failed. Based on the results, the authors have concluded that the internal cracks crucially influence the load carrying capacity. Moreover, based on results of a series of static bending, tensile and compressive tests on slightly cracked sleepers, the authors concluded that the PCSs are quite robust and small cracks do not significantly affect the load carrying capacity of sleepers. To investigate the residual strength, Kaewunruen and Remennikov (Kaewunruen & Remennikov, 2009a) conducted rail seat bending moment test before and after subjecting PCSs to 50 identical impact loads with a 50 year return period and a magnitude of about 500 kN. The results show that the sleepers that have been subjected to the impact loads tend to possess a large amount of reserved strength in spite of stiffness reduction due to “large cracks.”

Sýkorová et al. (Sýkorová, Bártová, & Štemberk, 2012) employed a fatigue damage function to calculate the reduction of sleeper stiffness due to cyclic loading. The calculations show that the modulus of elasticity decreases sharply during the first few hundred thousand of load cycles. The

strands due to diffusion of chloride ions is known as a significant cause of PCSs deterioration (Mohammadzadeh & Vahabi, 2011). The resistance of concrete to corrosion of reinforcement significantly depends on the permeability of concrete to water and chloride ions. Uncracked HSC is

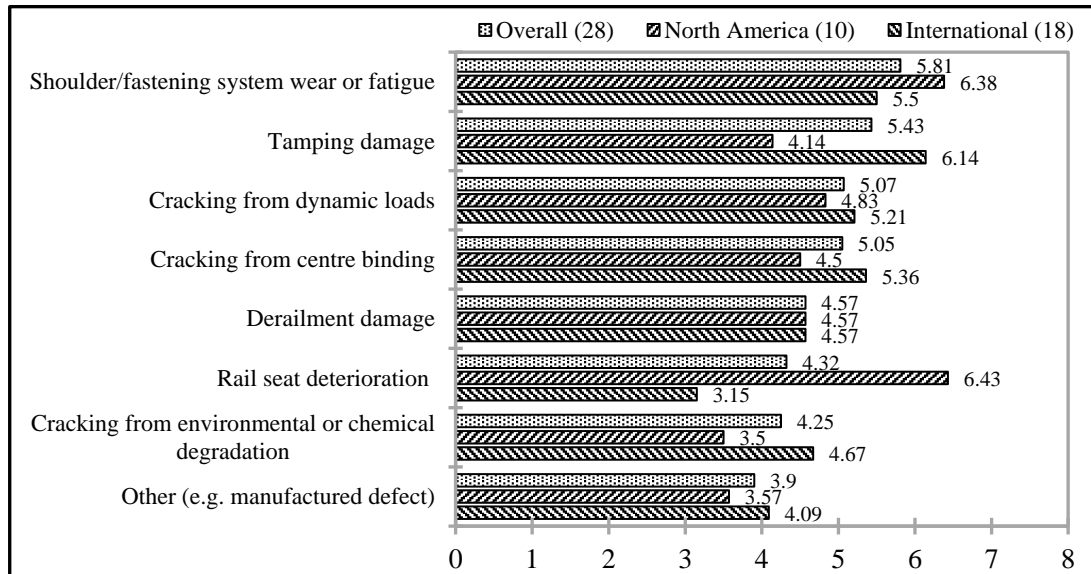


Figure 1. The most critical problem of PCSs and fastening system, ranked from 1 to 8 (adapted from (Van Dyk, Dersch, & Edwards, 2012))

authors believe that the fatigue behaviour of concrete under cyclic loads results in progressive and permanent changes in material and could cause micro-cracks within the sleeper, which, at times, appear as visible cracks on the surface. These calculations confirm the investigations by Gustavson and Gylltöft (Gustavson & Gylltöft, 2002) which show a 10 percent decrease in the flexural stiffness of sleepers because of cracking. While this reduction of stiffness has only small effect on the global response of the sleeper, cracks significantly influence the life span and may result in a high rate of corrosion or even fatigue failure of reinforcement.

In summary, low magnitude and high cycle service loads can only generate micro-cracks which result in stiffness reduction, but do not strongly influence the load carrying capacity of sleepers. In the case of repeated service loads together with stiffness reduction or occurrence of high magnitude and low cycle loads, cracks may propagate and appear visible. In extreme cracking cases, sleepers may fail and need early replacement.

2.2 Durability Effects

Generally, sleepers are utilised in various environmental conditions and are susceptible to penetration of water and diffusion of chloride ions which can lead to corrosion of strands. Corrosion of

expected to be less water permeable than NSC because of a denser texture. But Aldea et al. (Aldea, Shah, & Karr, 1999) have found that cracking changes the behaviour of concrete in terms of water and chloride permeability, and both NSC and HSC are affected by cracking. The influence of micro-cracks and visible cracks on the durability of concrete sleepers is a serious concern.

As demonstrated, micro-cracks occurrence at PCSs is unavoidable under service loads. Reviewing published literature, Francois and Arliguie (Francois & Arliguie, 1999) found that micro-cracks due to service loads increase the penetration of chloride ions and can shorten the service life of reinforced concrete. This finding has been confirmed by a series of laboratory tests conducted by Mohammed et al. (Mohammed, Otuski, Hisada, & Shibata, 2001). Test results indicate that the presence of cracks can cause significant corrosion of steel bars in concrete, regardless of crack size. In contrast, it is shown that when crack opening displacement (COD) is less than 50 microns under loading, the crack width has little effect on concrete permeability. For COD between 50 to 200 microns, the permeability of concrete increases rapidly and then increases steadily and less rapidly (Wang, Jansen, Shah, & Karr, 1997). Furthermore, macroscopic cracks, which are mostly probable in PCSs, have a detrimental effects on corrosion of reinforcement in prestressed concrete and the test

results show a doubling of crack width with time under cyclic loading can be expected (Nawy, 2010). It can be concluded that the presence of cracks, especially those with COD over 50 microns, facilitates penetration of chloride ions and water into concrete sleepers, which can accelerate the corrosion of strands. This can result in concrete deterioration which, in turn, shortens the service life of the sleepers, particularly when sleepers are subjected to corrosive or freeze-thaw environments.

3 STRAIN RATE ENHANCEMENT OF CONCRETE TENSILE STRENGTH

It is well recognised that strain (loading) rates have significant effects on the mechanical behaviour of concrete. By increasing the strain rate, the strength of concrete significantly increases in both compression and tension (Ngo & Mendis, 2009). However, it was found that compressive strength are not as sensitive to strain rate as tensile strength. In addition to strength, the modulus of elasticity of concrete significantly increases with the increasing strain rate. To present the dynamic increase in concrete strength, dynamic increase factor (DIF), i.e. the ratio between dynamic strength and static strength, is commonly used. For example, Figure 2 shows DIF of compressive and tensile strength in a strain rate value

comparison with NSC (Ngo, Mendis, & Whittaker, 2013).

Dynamic testing results suggest that the strain rate effects on both compressive and tensile strength of concrete-like materials become significant when the strain rate is beyond a transition strain rate, which is about $[10]^0 - [10]^1$ 1/s for tensile strength and $[10]^2$ 1/s for compressive strength, respectively (Lu & Li, 2011). The insensitivity of concrete-like materials to strain rates below around $[10]^0$ 1/s is attributed to the presence of free water inside the nano-pores of the material. At strain rates above the transition rate, dynamic strength increases dramatically due to other physical phenomena such as structural effects, inertia and heterogeneity. Employing a micro-mechanism model, Lu and Li (Lu & Li, 2011) investigated the influence of micro-cracks on tensile strength of concrete-like materials. It is reported that in the same strain rate, the tensile strength generally decreases with a decrease in the micro-cracks spacing. Moreover, for a fixed spacing of micro-cracks, the tensile strength decreases with micro-cracks size at low strain rates, but increases at high strain rates. It is also suggested that the increase of fracture energy in dynamic tension is caused by multiple micro-cracks, which take place within a short time and need a high energy input to create the fracture surface (Brara & Klepaczko, 2007).

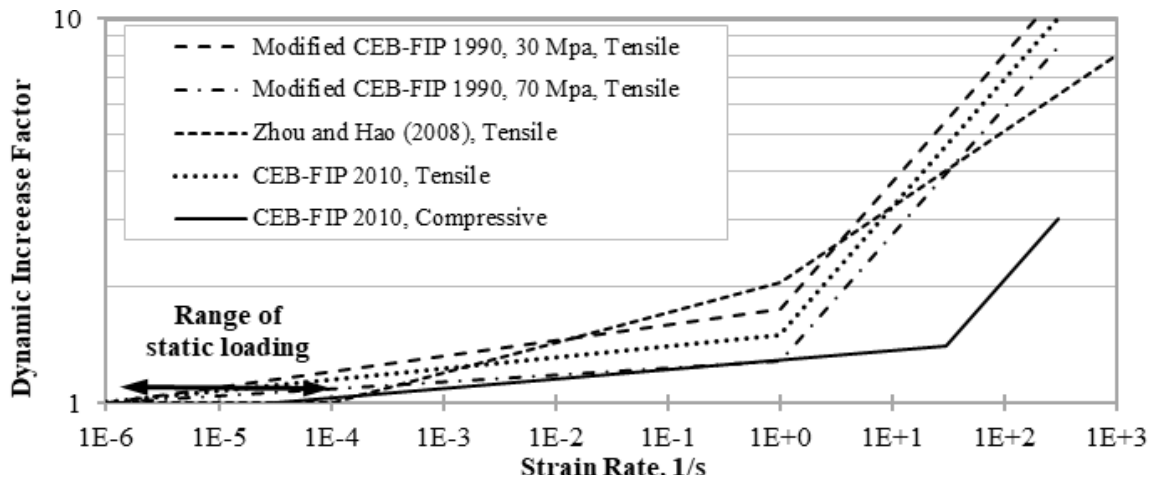


Figure 2. Influence of strain rate on compressive and tensile strength of concrete

between $[10]^{-6}$ and $[10]^3$ 1/s. Depending on concrete type and strain rate, DIF varies up to around 7.2. Similar graphs, presented by Ngo (Ngo, 2005), indicate DIF may reach values of about 2.2 and 1.6 for compressive strength and elastic modulus, respectively. Numerous investigations indicate that the response of concretes to strain rate depends on the static strength. It is demonstrated that the tensile strength of HSC is less sensitive to strain rate in

4 STRAIN RATES IN PCSS

The influence of loading rate on failure mode of PCSs was first investigated by Ye et al. (Ye, Wang, & Mindess, 1994). Although, they concluded that the cracking mode depends on the rate of loading and magnitude of impact, the effect of strain rate on the behaviour of concrete was unclear. Considering the strain rate and loading rate Wakui and Okuda (Wakui & Okuda, 1999) have suggested a simple technique to

investigate the ultimate capacity of PCSs to impact loads (as cited by (Kaewunruen & Remennikov, 2009a)). But the technique, which was based on

diagonal cracks. It is worth noting that the tests and estimations have been conducted based on three points bending moment on the rail seat.

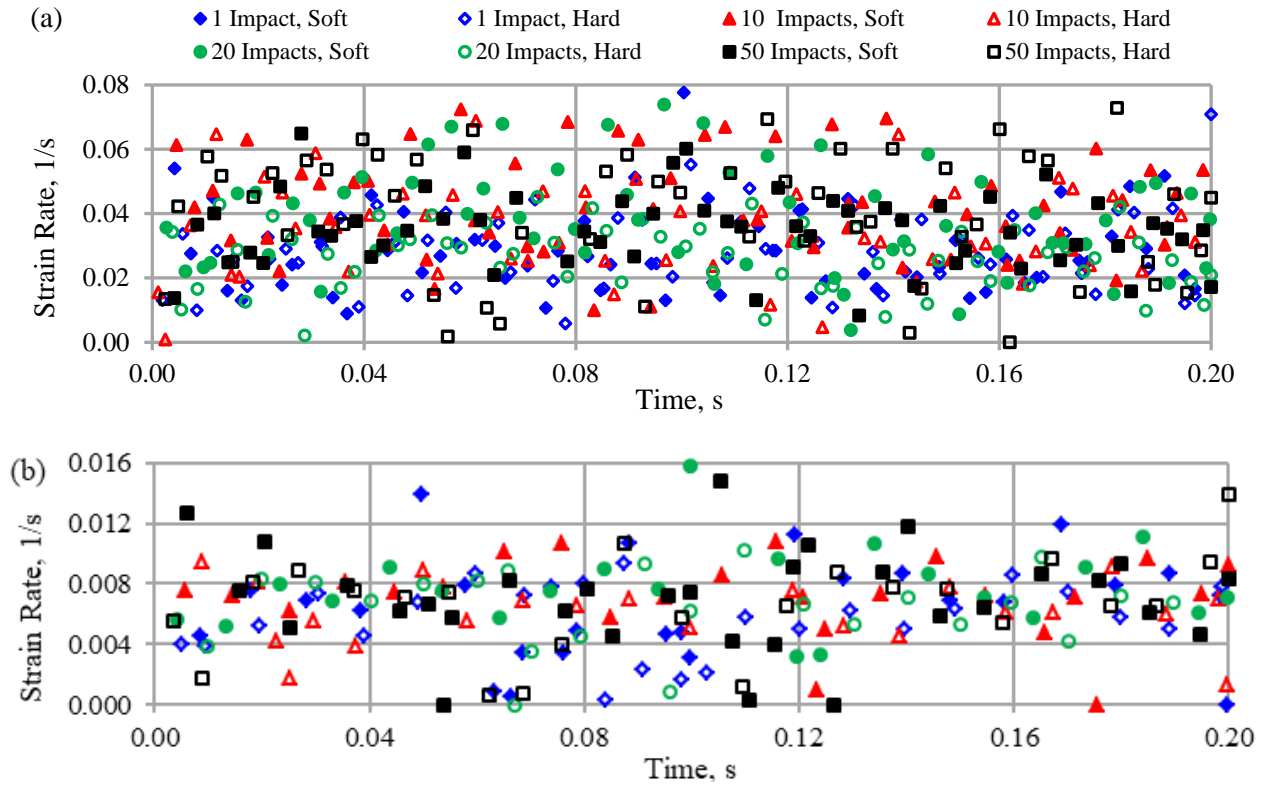


Figure 3. Calculated strain rates, (a) at rail seat and (b) at midspan

sectional analysis and only tendons failure mechanism, has been failed to approve.

To investigate the ultimate capacity of PCSs to impact loads, Kaewunruen and Remennikov (Kaewunruen & Remennikov, 2009a) calculated the dynamic compressive strength of concrete and dynamic yield stress of prestressing wires using logarithmic equations. The influence of strain rates has been considered in the equations. Further, they employed a high capacity dropping impact machine and carried out a series of impact tests on real scale PCSs. The duration and magnitude of impact loads have been recorded to estimate the strain rates at the concrete and prestressing wires. The ultimate dynamic strain of concrete and prestressing wires ($4.5 \times [10]^{(-3)}$ and $20 \times [10]^{(-3)}$, respectively), impact duration (4 ms) and stress wave delay, have been taken into account and the strain rates at the concrete and prestressing wires have been estimated as 2 and 6 1/s, respectively. Based on these rates the cracking moment of the sleeper at the rail seat has been predicted about 41 kN-m, which was 17 percent larger than static one. Also, the dynamic cracking moments that recorded during the experiment was 44 kN m, about 29 percent larger than that recorded during the static test. It appeared that the first cracks occurred due to bending, but the sleeper failed in the flexural-shear mode caused by the major

Based on the authors knowledge, there are no in-field measurements of strain rates at PCSs, published in the literature, to date. Recently, measurements of internal and external strains in PCSs have been reported by Grasse (Grasse, 2013) as a part of great investigation of PCSs and fastening system, but the results have not been published. The only measurements that can be used to estimate the strain rates were published by Kaewunruen and Remennikov (Kaewunruen & Remennikov, 2009b). The dynamic strain gauges were installed at the top and the bottom fibres around the rail seat and at the midspan of sleepers. Then the sleepers were subjected to multiple blows of impact force around 500 kN. Also, a thick rubber mat was used to replicate the ballast. Dynamic strain variations through time were recorded and reported after 1, 10, 20 and 50 blows of impact force in soft and hard track conditions. Altogether, 16 measurements were obtained. Unexpectedly, both positive and negative strains appeared in almost all measurements. Based on these measurements, Taherinezhad et al. (Taherinezhad et al., 2013) calculated the strain rates at both the rail seat and the midspan. The calculated strain rate magnitudes vary in the range of 0.01 – 0.08 1/s for rail seat and 0.002 – 0.016 1/s for midspan (see Figure 3).

Kaewunruen and Remennikov (Kaewunruen & Remennikov, 2009b) observed that the sleepers tend to have more cracks when subjected to multiple drop impacts. The cracks opened and became wider and larger, which could reduce the dynamic stiffness of sleepers. But, in regard to strain rates, calculations show no meaningful correlation between strain rate and number of impacts. Figure 4 shows the average values of calculated strain rates for the results of each experiment.

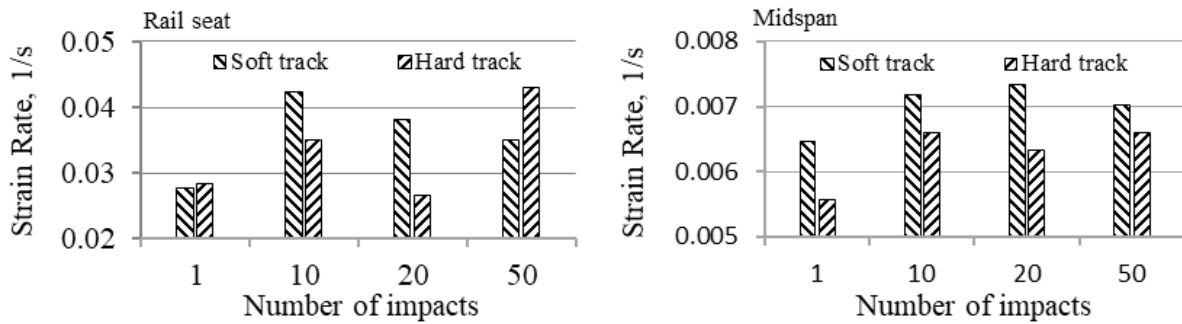


Figure 4. Average values of calculated strain rates under multiple impacts

5 CRACKING WHEEL LOADS OF PCSS

5.1 Specimens

To estimate loads which lead to crack initiation in PCSs, a sleeper section which is commonly used in Australia (with different lengths from 2.15 m to 2.85 m) has been investigated. Figure 5 shows the

accordance with AS 3600 (AS-3600, 2009) and suggested for HSC by Mendis (Mendis, 2001).

To compute the maximum stresses of concrete and strands at both rail seat and midspan of a sleeper, a computer program has been developed in accordance with Australia Standard (AS-1085.14, 2012). The ratio of the calculated stresses to the permissible counterparts has been restricted to a value of 1.05. Moreover, the calculated ballast pressure should not extend beyond 0.75 MPa for high-quality, scratch-

resistant ballast. The Standard prescribes quasi-static design procedure using the maximum axle load of the track as a design axle load. The vertical design wheel load is calculated by multiplying half of the axle load by a service factor which is used to account for the effects of wheel-rail dynamic interactions and to cover uncertainties related to the selection of the design axle load and its transfer to the rail seat of the sleeper. The Standard suggests a value of 2.5 for this service factor where in-field measurements are not

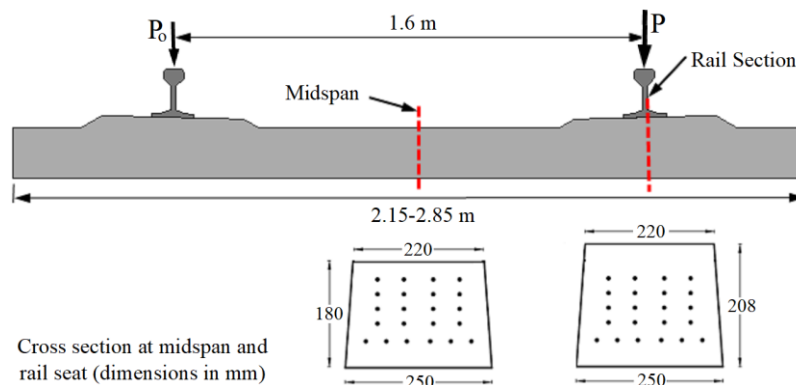


Figure 5. Sleeper dimensions

dimensions of the cross section at the rail seat and midspan plus locations of 22 prestressing strands with 5.03 mm diameter. It is worth mentioning that the gauge length is 1.60 m for these sleepers. This section was extensively studied by Kaewunruen and Remennikov at The University of Wollongong through the last few years. The characteristic compressive strength of concrete and the rupture strength of tendons were assumed 55 MPa and 1860 MPa, respectively. The tensile strength of concrete has been calculated using the equation $0.6\sqrt{f_c}$ in

available. Also, a load distribution factor is employed to calculate the vertical design rail seat load, depending on the distance between adjacent sleepers. In this article the distribution factor is about 60 percent, associated with a 0.75 m distance between sleepers, based on a graph presented in the Standard.

The length of the sleeper is optimised. The stress ratios and ballast pressure have been computed for increasing axle loads and a specific length of the sleepers. When one of the stress ratios reaches to the value of 1.05 or the ballast pressure reaches the value

loads, but two features have been included to consider the effects of rolling speed on the distribution factor and asymmetrical loading. Further, the service factor (2.5) has been reduced to 1.0 and calculated tensile stresses have been compared with the static tensile

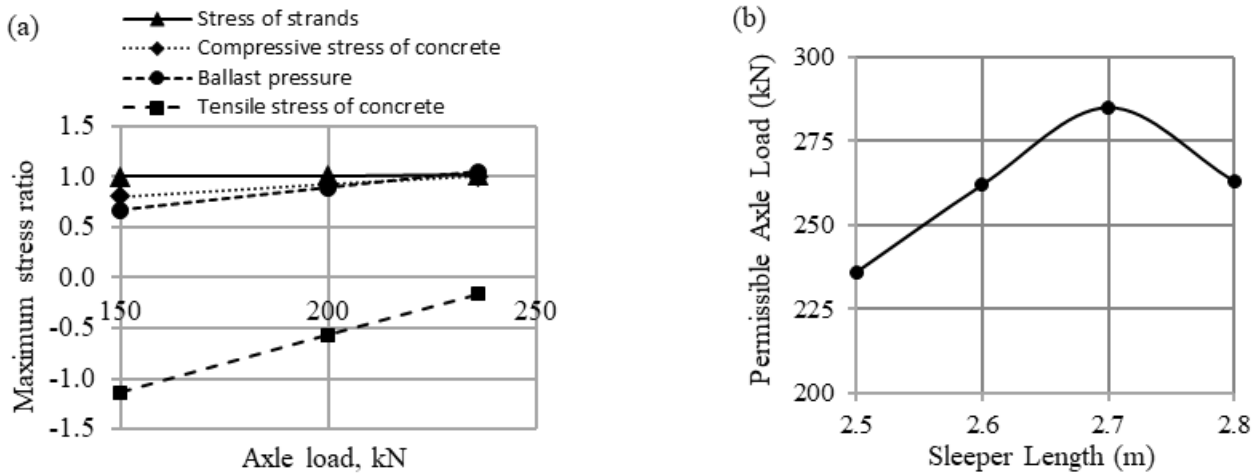


Figure 6. (a) The stress ratios for a sleeper length of 2.50 m, and 6(b) the permissible axle load of sleeper with different length

of 0.75 MPa, the related axle load is marked as the permissible axle load of the sleeper for that length. Figure 6(a) indicates the variation of stress ratios due to different axle loads when the length of sleeper is 2.50 m. The permissible axle load for the sleeper was found to be 236 kN. The graph also indicates that all four stress ratios vary linearly with increasing axle load. While the tensile stress of strands is far less sensitive, the tensile stress of concrete is highly sensitive to the load variations. Besides, the ratios of concrete tensile stress are negative for all of the load variations, which indicate that the concrete never experiences tensile stress even at the rail seat. This computation has been repeated for sleepers length of 2.60, 2.70 and 2.80 m. Similar trends are observed for sleepers with these lengths. However, the value of stress ratios for concrete tensile stress increases with increasing axle load, especially, in length of 2.80 m which exceed a value of 1.00. The permissible axle loads for different lengths of the sleeper are indicated in Figure 6(b). As shown in the graph, the permissible axle load reaches the maximum value when the length of sleeper is around 2.70 m. This length is hence the optimum length of the sleeper. The maximum magnitude of permissible axle load is about 285 kN. For this axle load the stress ratios are in the range of 1.02 to 1.05. 5.2

5.2 Cracking loads

For the next stage, a sleeper with 2.70 m length and 285 kN permissible axle load has been employed to estimate the load which leads to crack initiation. The computer program has been used again to calculate the tensile stress of concrete under different axle

strength of concrete instead of permissible tensile stress ($0.4\sqrt{f_c}$) specified by AS 1085.14 (AS-1085.14, 2012). According to Australian Standard, AS 3600 (AS-3600, 2009), the static tensile strength of concrete is obtained through the equation of $0.6\sqrt{f_c}$.

To investigate the influence of rolling speed on the distribution of wheel load on adjacent sleepers, Sadeghi (Sadeghi, 2010) undertook a lot of in-field measurements and found that the ratio of rail seat load to wheel load varies linearly with speed. While the ratio was around 0.57 for static conditions, it exceeds 1.0 for speed about 160 km/h. As the sleeper which is employed in this study is commonly used in heavy haul tracks, a value of 100 km/h was deemed to be a reasonable value for such kinds of tracks and high magnitude axle loads. Therefore, the value of distribution factor has been set to a constant value of 87 percent based on Sadeghi's investigations.

As previously mentioned, the high magnitude dynamic loads are generated due to wheel abnormalities or rail irregularities in the railway track. There is very low possibility for the simultaneous occurrence of abnormalities or irregularities on both sides of train or track. Consequently, the dynamic loads imparted to sleepers are largely asymmetric. The effects of large asymmetrical wheel loads on the response and failure of PCSs have been investigated by Kaewunruen and Remennikov (Kaewunruen & Remennikov, 2008). A finite element package STRAND7 has been employed to evaluate the bending moments of a sleeper at the rail seat and the midspan. The wheel load on the left hand side has been kept at a constant load of 100 kN (P₀) and the wheel load at the right

hand side (P) has been scaled by factors varying from 0.25 to 5.0. The authors have found that the bending moment at the least loaded rail seat would be redistributed to the higher loaded rail seat. The positive moment was found to increase linearly with increasing applied force P. Figure 7 shows the magnitudes of positive and negative bending moments plotted against different values of $[P/P]_0$. While the negative moment at midspan increases

experience tensile stress for large asymmetrical wheel loads.

There are several mathematical models reported in the literature to calculate the magnitude of DIF for concrete tensile strength due to strain rate such as those shown in Figure 2. CEB-FIP (CEB-FIP, 1993) modified models have been employed to consider the influence of strain rates on the concrete tensile strength. Two models for concrete with compressive

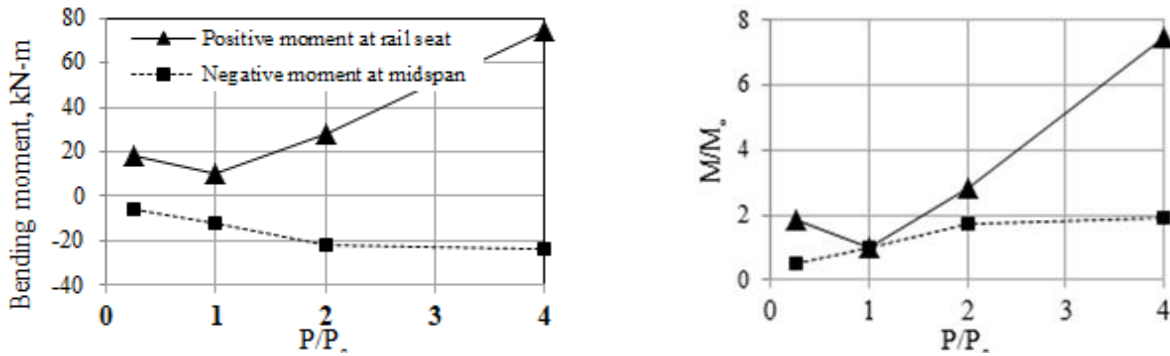


Figure 7. Bending moments versus $[P/P]_0$, (a) magnitudes and (b) ratios, adapted from (Kaewunruen & Remennikov, 2008)

slightly, the positive moment at the rail seat experiences a significant increase. Thus, the first cracks will most likely occur at the bottom of rail seat. The detection of those cracks is very difficult as they are not visible in a track environment due to the

strength of 30 and 70 MPa have been presented by CEB-FIP. It is considered reasonable to obtain the DIF for concrete with compressive strength of 55 MPa through interpolation between the two models, as both models are linear. It should be noted that the

Table 1. Tensile DIF and tensile strength of concrete at the rail seat and midspan

Position	Max strain rate, 1/s	Tensile DIF, CEB-FIP 1990			Tensile strength of concrete, MPa	
		30 MPa	70 MPa	55 MPa*	Static, $(0.6\sqrt{f'_c})$	Dynamic
Rail seat	0.08	1.60	1.23	1.37	4.45	6.10
Midspan	0.016	1.52	1.19	1.32	4.45	5.87

*Obtained through interpolation between two former columns.

existence of ballast. It is worth noting that the maximum negative moment tends to shift from the midpoint of sleeper to the side of the rail with the least loading.

The effects of rolling speed on the distribution factor and the influence of asymmetrical loading on the redistribution of positive and negative moments have been included in the computer program and the tensile stress ratios have been calculated. Figure 8(a) indicates that tensile stress at the bottom of rail seat considerably increases with increasing wheel load. As the tensile stress ratio reaches the value of 1.00 the cracks initiate, and the associated load is known as the cracking load. The results indicate that when the wheel load increases about 100 percent and reaches a value of 285 kN, the tensile stress ratio at the rail seat exceeds the value of 1.00 and flexural cracks initiate at the bottom. But, the tensile stress ratio at the midspan increases very slightly with increasing wheel load and remains negative, even for a wheel load with a magnitude of four folds of the permissible one. This means concrete at the top of the midspan does not

interpolated amounts are almost same as those suggested by CEB-FIP 2010 (CEB-FIP, 2010). Thus, the magnitudes of tensile DIF have been calculated for the maximum strain rates of 0.08 and 0.016 1/s, which occurred at the rail seat and midspan, respectively. Then, the dynamic tensile strength of concrete, which is the product of static tensile strength and tensile DIF, has been estimated, see Table 1.

The dynamic tensile strength of concrete has been included in the computer program and the stress ratios have been recalculated (Figure 8(b)). It appears that the tensile stress ratios at both rail seat and midspan follow the trends observed in Section 5.1, but the values of the stress ratios are slightly less for the same wheel load. When the wheel load increases to about 111 percent and reaches the value of 300 kN, the tensile stress ratio at the rail seat exceeds the value of 1.00 and flexural cracks initiate at the bottom. This is nearly 5.3 percent larger than the one obtained for static tensile strength. However, the ratio of tensile stress at the midspan remains negative even for very

high magnitude wheel loads. This means the midspan of sleeper does not experience tensile stress. Therefore, the concrete at the midspan remains uncracked.

6 PARAMETRIC ANALYSIS

The magnitude of the dynamic tensile strength of concrete, which is estimated based on the static compressive strength, depends on two main factors. The first factor is the equation that is used to calculate the static tensile strength, and the second factor is the model used to estimate the influence of strain rate. To further investigate cracking loads of PCSs, a new scenario has been examined to estimate the dynamic tensile strength of concrete.

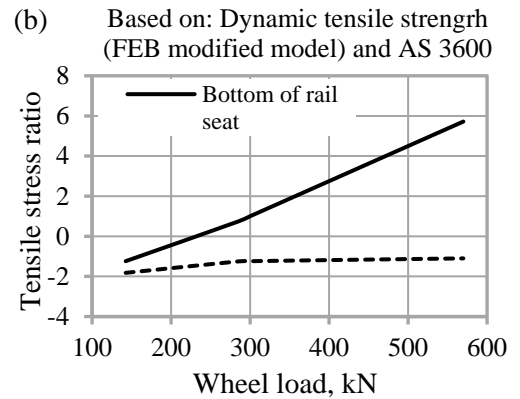
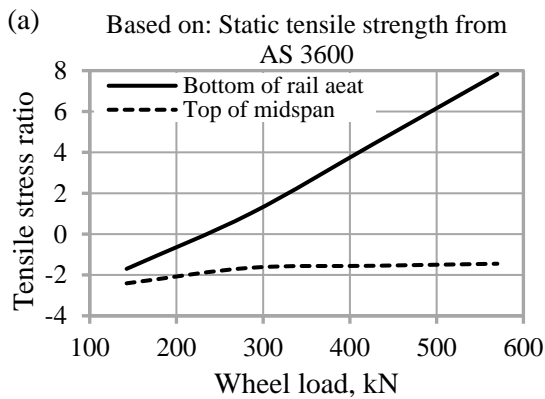


Figure 8. Tensile stress ratio of concrete versus different asymmetrical wheel loads

Hao, 2008) gives higher estimations for tensile DIF of concrete than other models, particularly, in the range of strain rates between $[10]^{-3}$ and $[10]^0$ 1/s. This model is shown in Figure 2. According to this model the values of DIF are 1.77 for rail seat and 1.59 for midspan which are about 29 and 20 percent higher than those estimated by modified CEB-FIP models (Table 2).

To include the outcomes from these models to the analysis, the computer program has been adjusted and the loads which cause initiation of cracks have been estimated. The results indicate that when the asymmetrical wheel load reaches the value of 359 kN, the tensile stress exceeds the dynamic tensile strength at the bottom of rail seat and the cracks tend to initiate. This load is about 26 percent higher than that appeared for static tensile strength (300 kN) and 20 percent higher than the cracking load estimated in Section 5.2. The stress ratios at both rail seat and midspan (Figure 9) are shown to follow the same trends as those observed in Section 5.1. 7.

7 DISCUSSION

The results indicate that bending cracks initiate at the rail seat bottom of an efficiently designed prestressed concrete sleeper when subjected to an asymmetrical wheel load with a magnitude about 2.1 to 2.5 folds of the permissible wheel load. Obviously, the cracks in this stage are micro-cracks and the size of cracks is not of a significant concern. However, the cracks will quickly propagate towards the top of the sleeper when the asymmetrical wheel loads increase. When the magnitude of the asymmetrical wheel load is three times of the permissible axle load, the tensile stress ratio can exceed the value of 1.6 to 3.2 depending on the scenario employed to estimate the dynamic tensile strength of concrete. Reviewing the published literature shows that depending on the

expand due to the large asymmetrical dynamic wheel loads that frequently occur in railway track as recorded and reported in the literature. More importantly, these cracks are invisible and very difficult to detect through an inspection scheme of the track.

As shown in Figures 8 and 9, the tensile stress ratio at the top of midspan always remains negative. This means that tensile stress does not occur at the midspan due to asymmetrical wheel loads even due those with higher magnitudes. However, cracking in this area have been reported in the literature, (see (Kaewunruen & Remennikov, 2008)). It seems that these cracks may occur due to large symmetrical loading. Two conditions, namely passage of overloaded trains and existence of unsupported (hanging) sleepers may contribute to the large symmetrical loads in a sleeper. To increase the profit margin, many train owners tend to overload the wagons, especially in recent years, as the capacity of freight trains is continuously increasing. Even vehicles with over 40 percent overload have been reported by Cheng et al. (Cheng, Harrison, Union, & Salient, 2007). However, this situation occurs very rarely. On the other hand, the existence of unsupported sleepers leads to a disturbance in

distribution of wheel load to adjacent sleepers. In this midspan varies very slightly with asymmetrical wheel

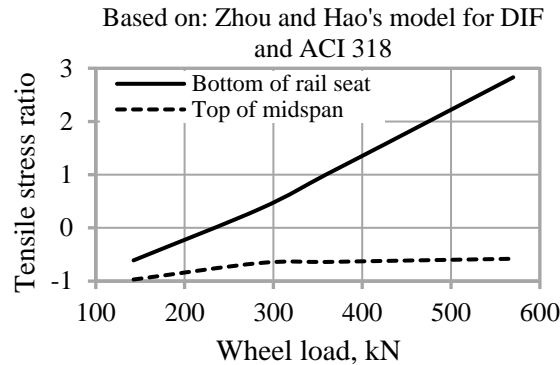


Figure 9. Tensile stress ratio of concrete versus different asymmetrical wheel loads

assumed monotonous, the results from the computer program show that about 40 percent overloading can cause the cracks to initiate at the top of midspan. The results indicate that by including the influence of strain rates to the analyzing process, the cracks at the bottom of rail seat initiate due to higher magnitude of loads which are about 5 to 26 percent higher than that estimated based on static tensile strength. This study supports the previous finding, published in the literature (Kaewunruen & Remennikov, 2009a) but, there is a crucial simplification in both studies, which is lack of the exact measurement of strain rates in PCSs at the track environment. Further, the dynamic tensile strength of concrete decreases when the cracks develop in terms of both size and numbers. In the other hand, the estimated strain rates at both rail seat and midspan are at the range that needs dynamic analysis according to load classification of CEB-FIP Model Code (CEB-FIP, 2010). It should be emphasized that the current study is a primary investigation of strain rate effects on PCSs and the strain rates have been estimated based on measurements at the laboratory. Consequently, it seems that better understanding of the strain rates effects on structural behaviour of PCSs require further investigation through in-field measurements, experimental works and numerical analysis.

8 CONCLUDING REMARKS

A prestressed concrete sleeper with a permissible axle load about 285 kN has been used to investigate the cracking loads under dynamic wheel load in this study. The effects of rolling speed on distribution of loads between adjacent sleepers and the influence of asymmetrical wheel loads on the bending moments at the both rail seat and midspan have been included in the study. The results indicate that the cracks at the bottom of rail seat initiate under a wheel load with a value of 285 kN, about 2 folds of the permissible wheel load. In contrast, the stress at the top of

suggested by (Zhou & Hao, 2008) have been applied instead. The results show that the cracks at the bottom of rail seat tend to initiate under wheel load about 300 and 359 kN, respectively, which are almost 5 and 26 percent larger than that obtained from static tensile strength of concrete. Further, the values of estimated strain rates reveal that PCSs require dynamic analysis based on load classification of CEB-FIP model code (2010). While, this study supports the previous published estimations, the current knowledge is not enough to come up conclusion now. Therefore, it is advisable that further in-field measurements, experimental works and numerical analysis should be undertaken to clarify the influence of strain rates on structural behaviour of PCSs.

REFERENCES

1. Aldea, C.-M., Shah, S. P., & Karr, A. (1999). Permeability of Cracked Concrete. *Materials and Structures*, 32(June), 370–376.
2. AREMA. (2006). *Manual for Railway Engineering*, Volume 1, Chapter 30, Ties. American Railway Engineering and Maintenance of Railway Association.
3. AS-1085.14. (2012). *Railway Track Material Part 14: Prestressed Concrete Sleepers*. Standards Australia Institute.
4. AS-3600. (2009). *Concrete Structures Australian Standard*. Standards Australia Institute.
5. Bian, J., Gu, Y. T., & Murray, M. (2013). Numerical Study of Impact Forces on Railway Sleepers under Wheel Flat. *Advances in Structural Engineering*, 16(1), 127–134. <https://doi.org/10.1260/1369-4332.16.1.127>
6. Brara, A., & Klepaczko, J. R. (2007). Fracture Energy of Concrete at High Loading Rates in Tension. *International Journal of Impact Engineering*, 34(3), 424–435. <https://doi.org/10.1016/j.ijimpeng.2005.10.004>
7. CEB-FIP, C. E.-I. du B. (fib). (1993). *CEB-FIP Model Code 1991 Design Code*. London, UK: Thomas Telford Services Ltd.
8. CEB-FIP, C. E.-I. du B. (fib). (2010). *Model Code 2010, First complete draft*. International Federation for Structural Concrete.
9. Cheng, L. R., Harrison, H., Union, W. G., & Salient, R. (2007). *Effects of Improper Loading in Heavy Haul*

- Operations. In *High Tech in Heavy Haul* (pp. 121–127). Kiruna, Sweden.
10. EN-13230-2. (2009). *Railway Applications - Track - Concrete Sleepers and Bearers - Part 2: Prestressed Monoblock Sleepers*. European Committee for Standardisation.
 11. Esveld, C. (2001). *Modern railway track* (2ed ed.). Delft University of Technology.
 12. Francois, R., & Arliguie, G. (1999). Effect of Microcracking and Cracking on the Development of Corrosion in Reinforced Concrete Members. *Magazine of Concrete Research*, 51(2), 143–150.
 13. Grasse, J. S. (2013). *Field Test Program of the Concrete Crosstie and Fastening System*. Universtiy of Illonois at Urbana-Champing.
 14. Gustavson, R., & Gylltoft, K. (2002). Influence of Cracked Sleepers on the Global Track Response: Coupling of a Linear Track Model and Non-linear Finite Element Analyses. *Journal of Rail and Rapid Transit*, 216(1), 41–51.
 15. Kaewunruen, S., & Remennikov, A. M. (2008). Effect of a Large Asymmetrical Wheel Burden on Flexural Response and Failure of Railway Concrete Sleepers in Track Systems. *Engineering Failure Analysis*, 15(8), 1065–1075. <https://doi.org/10.1016/j.engfailanal.2007.11.013>
 16. Kaewunruen, S., & Remennikov, A. M. (2009a). Impact Capacity of Railway Prestressed Concrete Sleepers. *Engineering Failure Analysis*, 16(5), 1520–1532. <https://doi.org/10.1016/j.engfailanal.2008.09.026>
 17. Kaewunruen, S., & Remennikov, A. M. (2009b). Impact Fatigue Responses of Pre-stressed Concrete Sleepers in Railway Track Systems. *The IES Journal Part A: Civil & Structural Engineering*, 2(1), 47–58. <https://doi.org/10.1080/19373260802479377>
 18. Leong, J., & Murray, M. H. (2008). Probabilistic Analysis of Train-track Vertical Impact Forces. *Proceedings of the ICE - Transport*, 161(1), 15–21. <https://doi.org/10.1680/tran.2008.161.1.15>
 19. Lu, Y. B., & Li, Q. M. (2011). About the Dynamic Uniaxial Tensile Strength of Concrete-like Materials. *International Journal of Impact Engineering*, 38(4), 171–180. <https://doi.org/10.1016/j.ijimpeng.2010.10.028>
 20. Lutch, R. H., Harris, D. K., & Ahlborn, T. M. (2009). *Prestressed Concrete Ties in North America*. In *AREMA Annual Conference* (pp. 1–39). Chicago, USA.
 21. Mendis, P. (2000). Softening of Normal Strength and High-Strength Concrete Frames. *Advances in Structural Engineering*, 3(2), 109–117. <https://doi.org/10.1260/1369433001502058>
 22. Mendis, P. (2001). *Design of High strength Concrete Members: State-of-the art*. Sydney, Australia: Engineers Australia.
 23. Mohammadzadeh, S., & Vahabi, E. (2011). Time-dependent reliability analysis of B70 pre-stressed concrete sleeper subject to deterioration. *Engineering Failure Analysis*, 18(1), 421–432. <https://doi.org/10.1016/j.engfailanal.2010.09.030>
 24. Mohammed, T. U., Otuski, N., Hisada, M., & Shibata, T. (2001). Effect of Crack Width and Bar Types on Corrosion of Steel in Concrete. *Journal of Materials in Civil Engineering*, 13(May/June), 194–201.
 25. Nairn, J., & Stevens, N. (2010). *Rational Design Method for Prestressed Concrete Sleepers*. In *Conference on Railway Engineering* (pp. 174–190). Wellington, NZ: Engineers Australia.
 26. Nawy, E. G. (2010). *Prestressed Concrete* (5th ed.). New Jersey: Prentice Hall.
 27. Ngo, T. (2005). *Behaviour of High Strength Concrete Subjected to Impulsive Loading*. The University of Melbourne.
 28. Ngo, T., & Mendis, P. (2009). Modelling the Dynamic Response and Failure Modes of Reinforced Concrete Structures Subjected to Blast and Impact Loading. *Structural Engineering and Mechanics*, 32(2), 269–282.
 29. Ngo, T., Mendis, P., & Whittaker, A. (2013). A Rate Dependent Stress-Strain Relationship Model for Normal, High and Ultra-High Strength Concrete. *International Journal of Protective Structures*, 4(3), 450–466.
 30. Okonta, F. N., & Magagula, S. G. (2011). *Railway Foundation Properties of Some South African Quarry Stones*. *EJGE*, 16(A), 179–197.
 31. Remennikov, A. M., & Kaewunruen, S. (2008). A Review of Loading Conditions for Railway Track Structures Due to Train And Track Vertical Interaction. *Structural Control and Health Monitoring*, 15(October), 207–234. <https://doi.org/10.1002/stc>
 32. Remennikov, A. M., Murray, M. H., & Kaewunruen, S. (2007). Conversion of AS1085 . 14 for Prestressed Concrete Sleepers to Limit States Design Format. In *AusRAIL PLUS* (pp. 1–18). Sydney, Australia.
 33. Sadeghi, J. (2010). Field Investigation on Dynamics of Railway Track Pre-Stressed Concrete Sleepers. *Advances in Structural Engineering*, 13(1), 139–152. <https://doi.org/10.1260/1369-4332.13.1.139>
 34. Sýkorová, J., Bártová, J., & Štemberk, P. (2012). *Prestressed Concrete Sleeper Under Extreme Loading Conditions*. In *18th International Conference Engineering Mechanics* (pp. 1281–1286). Svatka, Czech Republic.
 35. Taherinezhad, J., Sofi, M., Mendis, P., & Ngo, T. (2013). A Review of Behaviour of Prestressed Concrete Sleepers. *Electronic Journal of Structural Engineering*, 13(Special Issue), 1–16.
 36. Thun, H., Utsi, S., & Elfgrén, L. (2008). Load Carrying Capacity of Cracked Concrete Railway Sleepers. *Structural Concrete*, 9(3), 153–161.
 37. Van Dyk, B. J., Dersch, M. S., & Edwards, J. R. (2012). *International Concrete Crosstie and Fastening System Survey – Final Results*.
 38. Wakui, H., & Okuda, H. (1999). A Study on Limit-state Design for Prestressed Concrete Sleepers. *Concrete Library of Japan Society of Civil Engineers*, 30, 1–25.
 39. Wang, K., Jansen, D. C., Shah, S. P., & Karr, A. F. (1997). Permeability Study of Cracked Concrete. *Cement and Concrete Research*, 27(3), 381–393.
 40. Ye, X., Wang, N., & Mindess, S. (1994). Effect of Loading Rate and Support Conditions on The Mode of Failure of Prestressed Concrete Railroad Ties Subjected to Impact Loading. *Cement and Concrete Research*, 24(7), 1286–1298.
 41. Zhou, X. Q., & Hao, H. (2008). Mesoscale Modelling of Concrete Tensile Failure Mechanism at High Strain Rates. *Computers & Structures*, 86(21–22), 2013–2026. <https://doi.org/10.1016/j.compstruc.2008.04.013>
 42. Zhu, J. Y., Thompson, D. J., & Jones, C. J. C. (2011). On the effect of unsupported sleepers on the dynamic behaviour of a railway track. *Vehicle System Dynamics: International Journal of Vehicle Mechanics and Mobility*, 49(9), 1389–1408. <https://doi.org/10.1080/00423114.2010.524303>